ELSEVIER

Cement Based Cross-Ply Laminates

A. Pivacek, G. J. Haupt, and B. Mobasher
Department of Civil and Environmental Engineering, Arizona State University, Tempe, Arizona

A filament winding system was developed for manufacturing cross-ply cement based composites using continuous fibers. The computer-controlled system is used for manufacturing composite laminates, pipes, and pultruded sections. The electrical and mechanical components of the system are discussed in detail. Composite laminates are manufactured using continuous glass and polypropylene fibers. Their mechanical response is measured using closed loop uniaxial tensile and flexural tests. Results indicate that tensile strength of composites can exceed 50 MPa using 5% alkali-resistant glass fibers. By varying the stacking sequences, the ultimate strain capacity can be increased to more than 2% for glass fiber composites and 8% using polypropylene composites. The software/hardware system may be easily adapted for design and manufacturing of full-scale cement based composite laminate systems. ADVANCED CEMENT BASED MATERIALS 1997, 6, 144–152. © *1997 Elsevier Science Ltd.*

KEY WORDS: Fiber reinforced concrete, Cement composites, Laminated composites, Fibers, Toughness, Strength, Microcracking, Delamination, Mechanical testing

Development of new materials such as high performance fiber reinforced cement composites is guided by an understanding of the interaction between the portland cement based matrix, fibers, and interface characteristics. Despite years of research in the area of fiber reinforced cement (FRC) materials, their use as a structural material remains untapped. This is partly because low dosage addition of short fibers has merely increased the toughness as opposed to increasing the tensile strength of these materials. The goal of the present work is to develop processing techniques for manufacturing high performance materials for use as structural load bearing members, an area previously unattainable by conventional fiber reinforced concrete. These loading conditions may be defined through various impact, fatigue, shear, and multi-axial loading conditions.

A literature survey on the development of cement based composite systems was presented in an earlier work [1]. Using conventional processing techniques, FRC materials are traditionally made with a low-fiber volume fraction of short, randomly dispersed fibers. The fibers contribute to the toughness of the composite after the formation of the first crack. Beyond this level, it is assumed that the matrix does not significantly contribute to the strength of the composite material. With a higher volume of fibers, the microcracks can be controlled by arrest and bridging mechanisms. This allows the stresses to be transferred back into the matrix, forming more microcracks in the matrix material and considerably increasing the toughness. Once a certain volume fraction of fibers is exceeded, the ultimate strength and ultimate strain increase considerably. Theoretical approaches have demonstrated various mechanisms operative in increasing the strength, toughness, and fracture properties of the composites. The critical volume fraction of fibers necessary for distributed cracking has been studied by Li and Wu [2], Visalvanich and Naaman [3], Tjiptobroto and Hansen [4], Yang et al. [5], Li et al. [6] and Mobasher and Li [7]. These approaches concentrate on the toughening mechanisms in discrete fiber reinforced systems.

The work of Krenchel and Stang [8] showed that by using a high volume fraction of continuous fibers, the tensile strength of the composites may be increased significantly. By developing a manual pultrusion technique, they were able to develop composites containing up to 13% volume fraction of polypropylene fibers and a bend over point (BOP) of 15 MPa. The present study focuses on the development of processing and manufacturing techniques for composite laminates. Due to the significant strength and ductility improvement, these composites may prove to be the ideal choice for materials for new construction systems. Toughness and impact resistance may be increased dramatically. Test results are compared with the spray-dewatered glass fiber reinforced concrete (GFRC) panels reinforced with 5% randomly distributed short fibers. It is shown that pultruded FRC has a higher tensile and pseudostrain hardening response than conventional or extruded FRC materials [9].

The computer controlled manufacturing system that may be configured to make cross-ply and angle-ply laminates, pipes, and pultruded sections will be described briefly. We will also discuss the effect of ply

Address correspondence to: B. Mobasher, Civil and Environmental Engineering, Arizona State University, PO Box 875306, Tempe, AZ 85287-5306.
Received February 14, 1997; Accepted August 12, 1997

ISSN 1065-7355/97/$17.00
PII S1065-7355(97)00039-4

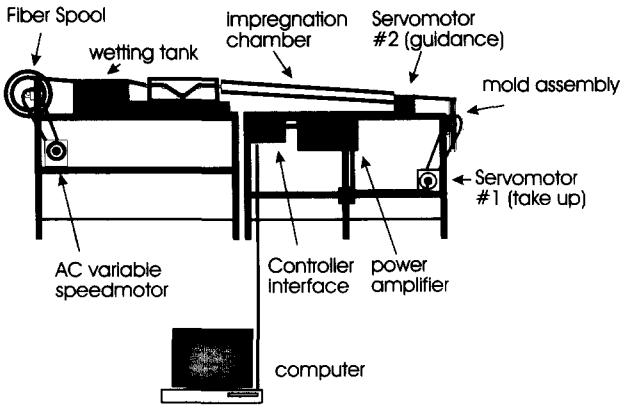

FIGURE 1. Schematic side view of the filament winding setup.

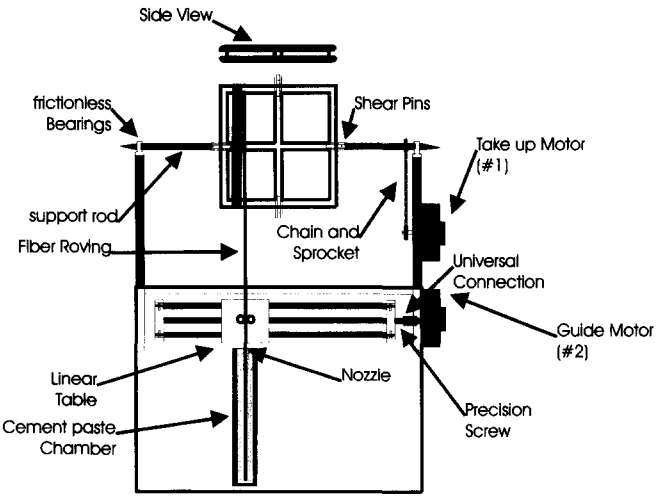

FIGURE 2. Schematic plan drawing of the take-up section.

orientation and stacking sequence on the mechanical properties under tensile and flexural loading.

The Filament Winding System

The mechanical components of the system shown in Figure 1 consist of the feed section, guide, and take-up (mold) sections. The electrical and electronics components consist of several servomotors, encoders, limit switches, and a computer. The computer uses object oriented programming language to monitor a closed-loop system that controls two servomotors. Configuration of the servomotors determines the winding, pulling, and guidance of the composites, while the take-up section controls the fiber (lamina) orientation [10].

Continuous fibers are used from a single spool and passed through a wetting tank. After the water is partially drained off, it is passed through an impregnation chamber. A manually adjustable speed control is used to provide the necessary torque to synchronize the rotation of the spool with the take-up section. The slurry infiltration chamber consists of a 1.5-m long tube that is cut in half lengthwise. This tube is filled with cement paste that impregnates the fiber along its travel path. The end of the tube rests on a platform that is mounted on a sliding table. This table moves transverse to the fiber direction. Two cylindrical posts on the platform align the fiber roving and control the volume fraction of the fiber as it exits the tube.

The sliding table with a travel range of 45 cm is shown in Figure 2. It is driven by a direct drive servomotor and guides the fiber roving onto the mold. An optical encoder measures the displacement, velocity, and acceleration of the drive shaft. The distance and speed of the servomotor controls the specimen width and the volume of fiber placed on the mold. Limit switches are installed at the two ends of the tables to terminate motion if necessary. A complete description of the mechanical and electrical set up is provided elsewhere [10,11].

The specimens are made in the take-up section by the winding process. The mold used for various 0, 90, and ±45 laminates is shown in Figure 3. It consists of two flat plexiglass plates 50 × 50 × 1 cm in dimensions separated by a 2.5-cm thick spacer block. The spacer block contains a series of guide slots with specific orientations, and its orientation can be easily changed during the winding process by switching the support rod from one guide slot to the other. The steel drive rod is tapered down to a conical shape at both ends so that as the mold is oriented the bar can pierce through the wound fibers. The mold assembly is chain driven by the second servomotor.

The main components of the electrical system are a 486 DX33 MHz computer, a servomotor controller, a servomotor amplifier, and a step-down transformer. The step-down transformer supplies the power to the

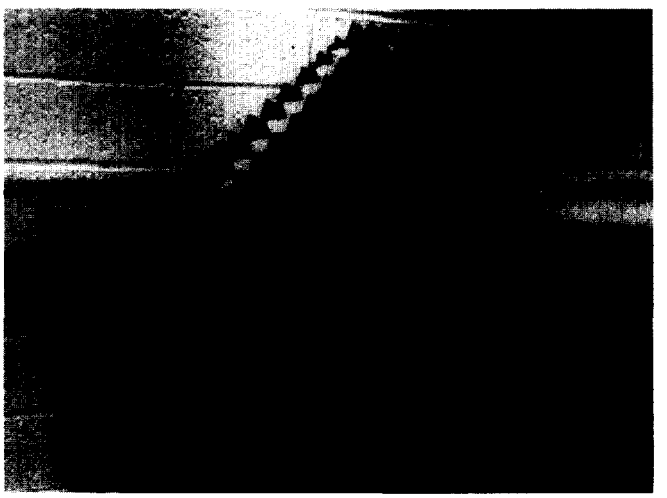

FIGURE 3. The mold used for various 0, 90, and ±45 laminates.

TABLE 1. Properties of AR glass and polypropylene fibers

Fiber	L_f (mm)	d_f (micron)	Ultimate Strength (MPa)	Elastic Modulus (GPa)	Density (g/cm^3)
AR Glass	Continuous	12	1725	70	2.70
Polypropylene	Continuous	35 × 250	340–500	8.5–12.5	0.91

amplifiers. The computer controls the operation through Labview®, an object oriented programming language that allows creation of different virtual instruments and their integration into a simulated control panel [12]. The servocontroller is capable of handling the motions of up to four axes using the feedback from their respective encoder. Additional capabilities include end of travel limit switches for clockwise and counter-clockwise motion.

Specimen parameters include the sample width, the layer orientation, and the ply thickness. These dimensions are converted to the distances and velocities of servomotors. The ply thickness depends on the velocity components of the two motors. For example, a uniaxial piece of certain thickness can be made in one slow pass or in several passes. The algorithm for making uniaxial continuous fiber composites consists of several passes along the guide section and switching the sign of guide distance as the servomotor stops at the end of each pass. To make cross-ply laminates, motion was paused after a pass to remove the axis bar and rotate the mold 90 degrees. The motion was then resumed. For a 0/90/90/0 sample, the guide speed can be reduced by half for the 90 degree pass to accomplish the desired thickness in a single pass.

Materials

The matrix formulation for all the specimens prepared in this study consisted of a mixture of 85% type I/II portland cement, 15% silica fume, and a water to solids ratio of 0.35. A superplasticizer was used to aid the rheology of the paste. The ingredients were mixed in a high-energy shear mixer for 5 minutes prior to use in the impregnation chamber. Table 1 presents the properties of alkali-resistant (AR) glass and polypropylene fibers used in the present study. The volume fraction of glass fibers in a lamina was between 4.8 to 9.6%. The volume fraction of fibers in polypropylene fiber reinforced concrete (PPFRC) specimens was 7%.

After the windings were completed, the mold was pressed at a constant pressure of 0.5 MPa under a hydraulic ram. The consolidation of the sample resulted in a reduced interlaminar porosity and removal of excess water. The pressure was maintained for 3 hours. The average thickness of a single ply was 5 to 6 mm, and the specimens were in the range of 20 to 25-mm thick. Samples were covered with polyethylene sheets and placed in a curing room at 90% relative humidity (RH) for 24 hours. All specimens were subjected to 28 days of curing in a saturated lime solution.

Mechanical Testing

Tension and flexural tests were performed using a closed loop servo-hydraulically controlled MTS 810 Material Test System (manufactured by MTS Systems, Minneapolis, MN) with a load capacity of 225 kN (50 Kips). The closed-loop testing was conducted with feedback controlling signals from linear variable differential transducer (LVDT) setups for axial strain in tension and deflection controlled for flexure. The time, stroke, load, and LVDT signals were collected using a data acquisition system with 12-bit resolution.

The closed-loop uniaxial tension tests were performed on 41 samples (36 AR glass and 5 polypropylene). Since tensile tests are influenced by the loading condition at the grips, dog-bone shaped specimens with cross sectional area of 50 × 20 mm at the reduced section were used. A set of hydraulic grips with serrated jaw-faces and capacity of 225 kN were used, resulting in fixed-end conditions. Gripping pressure was controlled at a range of 1.4 to 21 MPa by means of a manifold valve.

Two LVDTs located on opposite faces of the specimen monitored the elongation of a 90-mm gage length. The two signals were averaged and used as the feedback control for the closed-loop system. Placement of the LVDTs on opposite sides of the specimen reduced the bending effects due to frame misalignment or early single lamina failure. The LVDTs have a range of ±1.27 mm. The testing procedure started with a pre-load of 88 N, followed by LVDT control at a strain rate of 0.0005 mm/sec.

Four-point flexure tests were performed on 18 samples. The mid-span deflection was measured using a single LVDT and used as the control feedback signal. This setup eliminated support settlement or seating problems as well as specimen rotations. A spring loaded LVDT with a range of ±2.54 mm was used to control the test as the feedback signal. Tests were conducted at a 0.005 mm/sec. displacement rate.

Analysis of Test Results: Uniaxial Tension Tests

Glass Fiber Laminates

In most FRC composites with short randomly dispersed fibers at a low volume fraction, the matrix phase does

TABLE 2. Tensile test response of unidirectional and cross-ply AR glass (G) and polypropylene (PP) composites

Lay-up	No.	V_f (%)	E (GPa)	E_2 (GPa)	σ_{BOP} (MPa)	ϵ_{BOP} (mm/mm)	$\sigma_{ultimate}$ (MPa)	$\epsilon_{ultimate}$ (%)
0 G	10	4.8	22.33	9.15	12.06	0.92E-3	45.22	0.82
0/90/0 G	4	4.8	8.46	2.82	6.91	1.41E-3	21.81	1.25
$(0/90)_s$ G	5	5.0	21.63	1.89	9.86	2.39E-3	38.27	1.84
90/0/90 G	4	5.0	11.31	2.47	11.58	1.27E-3	34.29	1.41
$[45/-45]_s$ G	3	9.6	1.354	—	0.77	0.96E-3	5.12	0.48
$[0/-45/45]_s$ G	3	5.6	14.23	—	5.35	0.40E-3	44.20	1.35
$[0/-45/45/90]_s$ G	3	8.8	17.14	—	9.71	0.56E-3	50.32	1.22
PP 0	5	7.0	22.50	0.22	7.80	0.90E-3	14.02	3.94

Subscript s stands for symmetry in plies $(0/90)_s$ = (0/90/90/0).

not contribute to the overall strength of the composite until the first cracking takes place. With a higher volume of closely spaced fibers, the microcracking can be controlled by crack arrest and bridging mechanisms [13]. This allows the stresses to be transferred back into the matrix, forming additional microcracks while considerably increasing the toughness. Once the critical volume fraction of fibers is exceeded, the ultimate strength and ultimate strain increase considerably [14].

Several parameters characterize the tensile response. These include the modulus of elasticity (E), first cracking strain, BOP, and the slope in the quasilinear region beyond the BOP defined as E_2, the pseudo strain hardening region, ultimate strength, and the toughness. Test results of uniaxial cross-ply and angle-ply laminates are presented in Table 2.

The typical stress-strain curve of tensile tests for unidirectional and $(0/90/0)_s$ specimens is shown in Figure 4. Test results are compared with the tensile response of plain mortar reinforced concrete and GFRC,

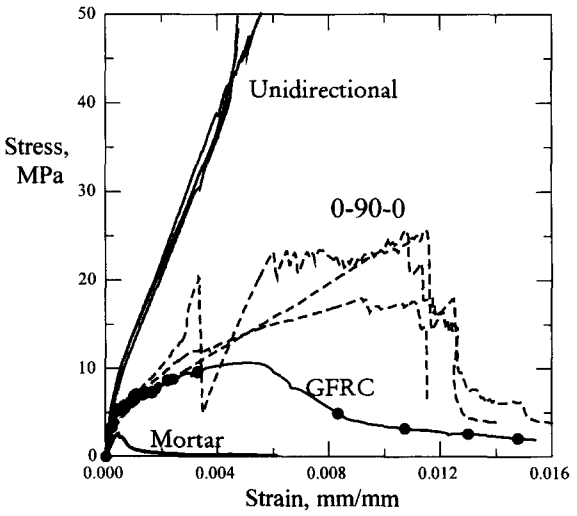

FIGURE 4. Tensile stress-strain curve of unidirectional and 0/90/0 specimens compared with glass fiber reinforced concrete and mortar.

which utilizes approximately 5% chopped randomly distributed glass fibers [15]. It is noted that the tensile response is significantly improved with the present manufacturing technique. By comparing the unidirectional fiber composites with the GFRC sample, it is observed that the efficiency of fiber length and alignment is represented by a five-fold increase in the ultimate tensile strength. The initial response of the composites is linear up to the BOP. The experimentally obtained E of the composite for the uniaxial and $(0/90)_s$ specimens are close to the expected values from the rule of mixtures and by other models [16]. The initial stiffness values for 0/90/0 and $(90/0)_s$ composites were lower than the theoretical values, which may be attributed to the lack of proper bond and the rotation of the specimen in the grips.

The BOP level represents the transition from linearity and begins with the formation of an isolated crack and ends when it has propagated across the entire width of the specimen [17]. The most notable discrepancy from conventional short random fiber reinforced cements (SRFRC) is that the BOP level is characterized by a smooth transition from the primary to the secondary linear response. The reason for the gradual transition instead of an abrupt change in slope is that the fibers delay the localization by transferring stresses back into the matrix. The uniform placement of the glass fibers within the matrix mobilizes them fast enough to smooth out the very distinct BOP. It is also shown that the load increases over a large level of strain as the matrix cracking continues. The Aveston, Cooper, and Kelly model predicts that this will happen at a constant load level over a large strain range [18], whereas in the present composites, cracking seems to be continuous.

Following the transition of the stress into the pseudostrain hardening state, the stiffness of the unidirectional composites may be easily compared with the contribution of the fiber in terms of E_fV_f, or 3.75 GPa (under assumed values of E_f = 75 GPa and V_f = 5%). On average, the uniaxial samples had a secondary slope (E_2) of 9.15 GPa, more than twice the expected value.

This represents the contribution of the matrix phase in stiffening the composite. The E_2 values signify that the matrix is still carrying a portion of the applied load, although it has undergone a large amount of strain and cracking. In the cross ply composites, this stiffness level (E_2) was computed at approximately 50 to 75% of the expected value computed by means of ply discount method. This is expected because the 90 degree layers have no load carrying capabilities due to cracking of the matrix.

The cross-ply composites exhibited much larger ultimate strain capacities than the uniaxial specimens. This higher level of strain capacity was also associated with a reduced ultimate strength level. Almost all cross-ply composites showed ultimate strains in the range of at least 1% and up to 4%. The average ultimate strain values increased 124% for $(0/90)_s$ samples while the 90/0/90 and $(90/0)_s$ composites increased 71% and 52% when compared with the uniaxial samples. BOP strains were also much larger, with $(0/90)_s$ composites being 260% larger than the uniaxial samples. The cross-ply composites experienced a drop in ultimate strength when compared with uniaxial specimens. The $(0/90)_s$ composites had an average ultimate strength of 38.27 MPa or 15% lower than the uniaxial composites. At the higher strain levels, only the 0 degree plies carried the load in cross-ply composites. It was observed that the majority of the cross-ply composites exhibited a tensile strength value above 30 MPa, with an ultimate strain over 1%. This added ductility is attributed to the cracking of the 90 degree plies over the entire specimen length.

The failure mechanism of cross-ply composites was characterized by formation of intralaminar cracks, which formed parallel to the loading direction along the specimen width. These cracks formed at the 90 degree layers and grew toward the 0 to 90 degree interface, resulting in debonding of the laminates. This mechanism was the major mode of failure in the cross-ply composites. The failure of the 90 degree layers resulted in an increased stress in the 0 degree layers. Ultimate strengths in four uniaxial and one $(0/90)_s$ specimen exceeded 50 MPa, two of these having ultimate strains over 1.2%. It was observed that variations in the failure modes were influenced by the gripping parameters. Testing conditions may influence the ultimate strength of the composite.

One of the ways to reduce the interlaminar shear between the highly orthotropic 0 and 90 degree layers is to incorporate a 45 degree layer between them. In order to observe the effects of such a modification, the mechanical response of a ±45 degree laminate is observed first in Figure 5, which represents the tensile response of a four-ply $(\pm 45)_s$ composite. Although the initial portion of the response is linear, the linearity is terminated well below the range observed in other composites (10 to 30 MPa). With the fibers at a 45 degree orientation, only half of the applied stress is directed along the fiber axis, while the other half results in shear stresses causing fiber delamination. Due to the low strength of the fiber-matrix bond, cracks that are oriented at 45 degrees to the loading direction form at the fiber/matrix interface. This may be partly attributed to the lack of complete impregnation of the fiber roving and formation of several inherent weak spots leading to low tensile strength.

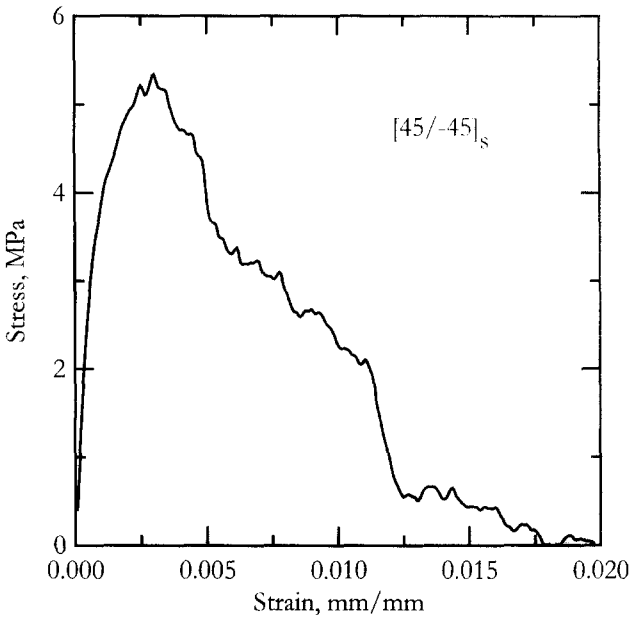

FIGURE 5. Tensile stress-strain response of a $(\pm 45)_s$ composite.

The mean ultimate strength was 5.6 MPa at 0.25% strain. This represents a value equal to 13% of the average ultimate strength for uniaxial specimens. Beyond this level, one major inclined crack was formed along the fiber's axis, leading to failure of the composite. Due to lack of fibers bridging the crack along this direction, redistribution of the stresses was not possible. Since no other cracking was observed in the outermost layer, it may be assumed that this strength represents the transverse bond strength of the fiber and matrix.

Addition of a 45 degree lamina between cross-ply laminates can substantially decrease the shear stress as shown in Figure 6. In an "as-is" condition, a ±45 degree layer contributes a marginal amount to the load carrying capacity of the composite. When placed between the 0 and 90 degree layers, it is observed that the nominal strength of the composite is significantly improved compared with a unidirectional or $[0/\pm 45]_s$ composites. The role of the 45 degree layers is therefore to reduce the interlaminar shear stresses and allow for a

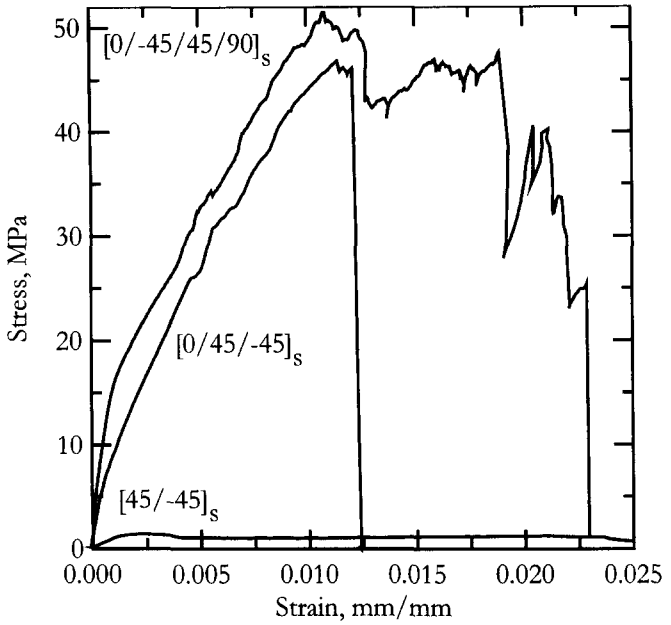

FIGURE 6. Effect of ±45 layers on the tensile load carrying capacity of the composites.

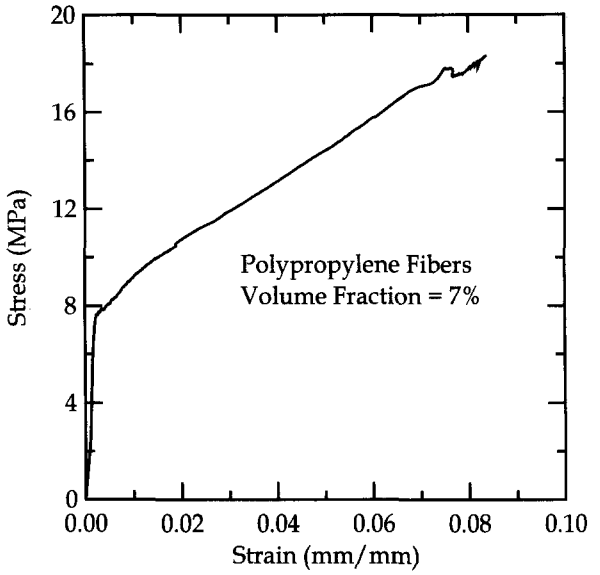

FIGURE 7. The stress-strain response of a polypropylene fiber composite containing 7% fibers.

better distribution of the cracking in the composite. As shown in Figure 6, the tensile stress strain curve of a $[0/-45/45/90]_s$ composite is characterized by an ultimate tensile strength of 50 MPa and an ultimate strain capacity of more than 1%. Examination of the postpeak response indicates a far superior performance compared with uniaxial fiber composites. The extent of cracking in these composites is indicative of the ability of the 90 degree layer to distribute the microcracks throughout the matrix phase while the 45 degree layers tend to reduce the shear stresses between the plies. Even at 2% axial strain, the load carrying capacity remains significantly high.

Polypropylene Fiber Laminates

Polypropylene fiber composites were filament wound into uniaxial specimens. Figure 7 represents the tensile stress-strain response of composite containing 7% polypropylene fibers. The stress-strain curves are in agreement with the results of manually pultruded composites tested by Krenchel and Stang [8] and Mobasher, Stang, and Shah [17]. As shown in Figure 7, the straining was continued up to 8% strain level. The stress-strain response is semi-linear up to approximately 8 MPa, and ends with a very distinct BOP. The BOP stress value is dependent on volume fraction of fibers, water/cement ratio, and bonding efficiency of the fiber-matrix interface. The modulus of elasticity value is well within the predicted range of rule of mixtures and represents the matrix properties, especially since the fiber modulus is weaker.

The multiple cracking phase, signified by the increasing strain at a reduced stiffness, follows the BOP. This phase ends as the cracking is saturated in the specimen, and the composite stiffness depends on the contribution of fibers only. The theoretical E_fV_f value for polypropylene fibers (E_f = 7.0 "initial" GPa and V_f = 7%) is 0.49 GPa, while the secondary slope is experimentally obtained as only 0.22 GPa. This variation depends on the bonding of the fibers to the matrix, the viscoelastic properties of the fiber.

Even when the specimen is loaded up to 8.5% strain, a stress level of 18 MPa is resisted. Formation of visible cracks parallel and transverse to the fiber direction was noted. This observation was later confirmed through microscopic evaluations of thin sections. Due to the saturation of cracking in the specimen at this stage, the majority of the load was being carried by the fiber phase only. Both the stress and strain levels were still rising at the termination of the test.

Flexural Test Results

Flexural testing of AR glass/cement specimens in four point bending was conducted. Twelve uniaxial specimens and six $(0/90)_s$ specimens were tested. Linear elastic behavior was assumed in the calculation of flexural properties. The proportional elastic limit (PEL) is considered the point at which the flexural stress-deflection curve deviates from linearity. The modulus of rupture (MOR) was computed based on elastic section properties. Flexural test results are shown in Table 3.

Flexural stress-deflection curves for several unidirec-

TABLE 3. Summary of the flexure test results

Lay-up	No.	E_c (MPa)	σ_{PEL} (MPa)	d_{PEL} (mm)	σ_{LOP} (MPa)	d_{LOP} (mm)	σ_{MOR} (MPa)	d_{MOR} (mm)
0	12	16.75	11.15	1.05	48.20	4.61	49.78	5.36
$(0/90)_s$	6	22.82	13.81	0.62	20.71	2.03	23.24	11.37

d = deflection.

tional fiber composites are shown in Figure 8. Note that the majority of the composites fail at an equivalent flexural stress above 50 MPa. The postpeak response, however, is varied because it depends on the nature of delamination failure and shear cracking in the composites. The flexural E is observed to be in the range for values for glass/cement composites containing random fibers. A thinner section could provide a higher flexural modulus response. Figure 9 represents a comparison between the unidirectional fiber composites and $(0/90)_s$ specimens containing 4.8% AR glass fibers with the portland cement paste. Addition of the fibers increases the strength of the composite by an order of magnitude. The postpeak ductility of the unidirectional composites is lower than the $(0/90)_s$ composites.

The PEL traditionally represents loss of linearity due to the formation of the first crack. This value is used for design of FRC materials. In the flexural stress-deflection curves, the PEL is not evident because there is only a slight change in the slope of stress-deflection response. This results from cracking being distributed with aligned continuous fiber composites. The PEL had an average value above 11 MPa for uniaxial samples and 13.8 MPa for $(0/90)_s$. These values are above PEL values previously obtained of 7.2~9.0 MPa [19]. The deflection at PEL was nearly 1 mm for majority of the uniaxial specimens and 0.85 mm for $(0/90)_s$. This is well above the deflection values of SRFRC with glass fibers of 0.18 mm [20]. The pseudolinear response of the flexural stress-deflection curve exists up to the 40 MPa in most cases. The specimen in the stage from the PEL to the peak level exhibits a much stiffer response than SRFRC composites. It is difficult to distinguish this stage from the initial response in all tests. This illustrates the increased efficiency obtained by proper fiber alignment and placement.

Beyond the PEL level, the first major cracking in the composites is referred to as the limit of proportionality (LOP). The LOP signifies the first permanent material damage and is synonymous to BOP level in tension. The average values for the LOP are presented in Table 3. The average deflection at the LOP for $(0/90)_s$ composites was less than one half the deflection of uniaxial composites. Four of the uniaxial specimens tested to the end of the LVDT range of 2.5 mm showed little to no permanent damage once load was removed, with no noticeable permanent deflections. The MOR was significantly higher than previous studies [15,16,21]. The uniaxial specimens were as much as two times stronger than the SRFRC values, while the $(0/90)_s$ were slightly higher.

The definition of toughness in brittle matrix compos-

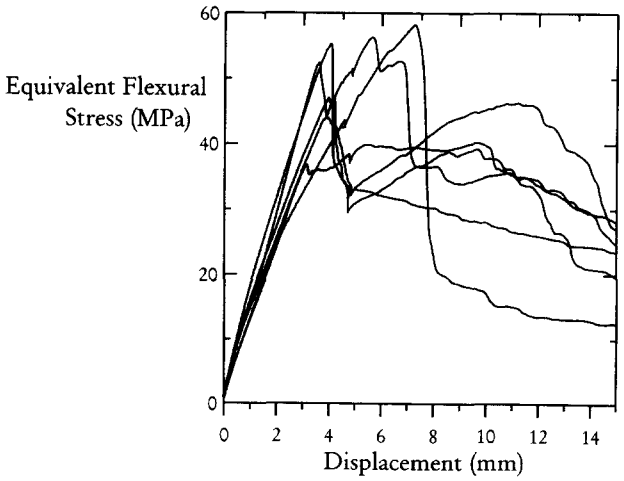

FIGURE 8. Flexural stress-deflection curve of uniaxial and 0/90/0 specimens containing 4.8% AR glass fibers compared with portland cement paste.

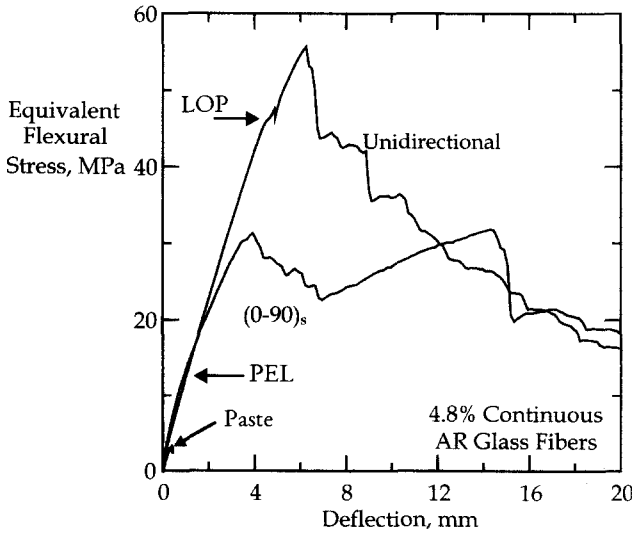

FIGURE 9. Flexural stress-deflection curve of uniaxial and 0/90/90/0 specimens containing 4.8% AR glass fibers compared with portland cement paste.

TABLE 4. Summary of toughness data for various composites

	Toughness (N/mm)		
Type	MOR	1%ϵ	Test end
0 T-G	—	—	16.08
$(0/90)_s$ T-G	—	16.42	42.49
0/90/0 T-G	—	12.30	14.94
$(90/0)_s$ T-G	—	15.73	27.96
$(\pm 45)_s$ T-G	—	3.26	3.77
0 T-PP	—	7.57	24.70
0 G-F	12.62	—	44.90
$(0/90)_s$ G-F	13.42	—	28.26

T = tension sample, F = flexure sample, G = AR glass, PP = polypropylene

ites varies widely. Results of toughness measurements are shown in Table 4. The tensile toughness was defined as the area under the stress-stain curve. The ultimate toughness values may not represent the material property since the failure mechanisms were quite diverse. Tests were terminated due to formation of longitudinal cracks along the neck region of the dog-bone samples or shear cracking induced by the gripping pressure. A higher level of energy absorption was observed for the cross-ply laminates. The formation of large transverse cracks in the 90 degree layers and their coalescence into major delaminations accounted for this behavior. Figure 10 represents the type of ply delamination cracking observed in a flexural specimen. The $(\pm 45)_s$ specimens exhibited a low toughness, approximately one fifth of the uniaxial composites. This behavior was expected since fiber orientations were aligned in an off axis direction.

The uniaxial polypropylene specimens absorbed a higher amount of energy than the glass specimens. This is due to the extended strain range of polypropylene

FIGURE 10. Ply delamination cracking observed in a flexural specimen (scale markers represent 1 mm).

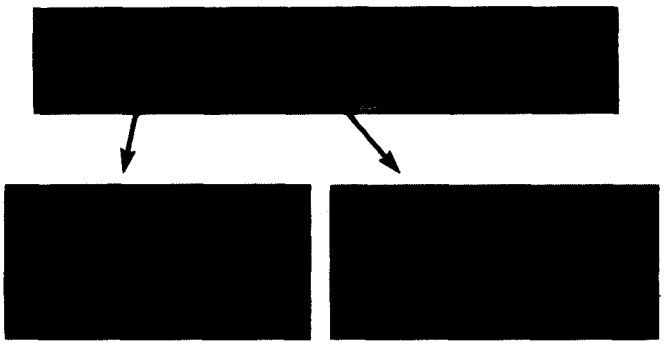

FIGURE 11. Delamination microcracking in a 0/90/90/0 AR glass fiber composite subjected to tension.

fibers. At the strain level 8.5% strain, an approximate amount of 108 N/mm was absorbed.

The toughness of flexural samples was measured as the area under the load-deflection curve divided by the cross sectional area. The uniaxial specimens had the highest energy absorption capacity, while the $(0/90)_s$ specimens formed delamination cracks after the formation of transverse cracks in the 90 degree layers (Fig. 11). Compared with short fiber composites, the flexural toughness of aligned-fiber laminates dramatically increased. Although the toughness is normally viewed as the work to fracture, many specimens failed to achieve a complete fracture.

Conclusions

Cement based composite laminates were manufactured using a filament winding system. Mechanical response of composite laminates was measured using closed-loop uniaxial tensile and flexural tests. Results indicate that tensile strength of composites can reach in excess of 50 MPa. The weak phase in cross-ply composite laminates is the ply interface layer. Distributed cracking in the 90 degree plies results in toughening of the composites and the strain capacity is improved significantly. Addition of a symmetric layer at 45 degrees was observed to provide significant stress redistribution. It was observed that cross-ply composite laminates with 5% AR glass fibers may carry in excess of 35 MPa at strain levels as high a 2%.

Acknowledgements

Support of the National Science Foundation through the research initiation award #MSM-9211063, Program Director Dr. K. P. Chong, is greatly appreciated.

References

1. Mobasher, B.; Li, C.Y. Saadatmanesh, H.; Ehsani, M.R., Eds. *Proceedings of the First International Conference for Composites in Infrastructure*; Tucson, AZ, 1996; pp 123–136.

2. Li., V.C.; Wu, H.C. *J. Appl. Mech. Rev.* **1992,** (8), 390–398.
3. Visalvanich, K.; Naaman, A.E. *J. of American Concrete Institute* **1983,** (2), 128–138.
4. Tjiptobroto, P.; Hansen, W. *ACI Mat. J.* **1993,** (1), 16–25.
5. Yang, C.C.; Mura, T.; Shah, S.P. *J. of Mat. Res.* **1991,** *6*(11), 2463–2473.
6. Li, S.H.; Shah, S.P.; Li, Z.; Mura, T. *Int. J. of Solids and Structures* **1991,** *30*(11), 1429–1459.
7. Mobasher, B.; Li, C.Y. *ACI Materials Journal* May-June **1996,** *93*(3), 284–292.
8. Krenchel, H.; Stang, H., In *Brittle Matrix Composites 2*; Brandt, A.M.; Marshall, I.H., Eds.; Elsevier Applied Science: Poland, 1994; pp 20–33.
9. Shah, S.P.; Shao, Y.; Li, Z. In *Brittle Matrix Composites 4*; Brandt, A.M.; Li, V.C.; Marshall, I.H., Eds.; Woodhead Publishing Ltd: Cambridge, Eng., 1994; pp 17–26.
10. Pivacek, A. MS Thesis, Arizona State University, May 1997.
11. Mobasher, B.; Pivacek, A. *Journal of Cement and Concrete Composites* **1997,** in press.
12. *LabView Version 4.0, Users Manual*; National Instruments Inc.; Austin, TX, 1996.
13. Li, C.Y. Doctoral Dissertation, Arizona State University, May 1995.
14. Balaguru, P.N.; Shah, S.P. *Fiber-Reinforced Cement Composites*; McGraw-Hill Inc.: New York, 1992.
15. Mobasher, B.; Shah, S.P. *ACI Materials Journal*, Sept.-Oct. **1989,** 448–458.
16. Brandt, A.M. *Cement Based Composites: Materials, Mechanical Properties, and Performance*; E & FN Spon: London, 1995.
17. Mobasher, B.; Stang, H.; Shah, S.P. *Journal of Cement and Concrete Research* **1990**, 665–676.
18. Mallick, P.K. *Fiber-Reinforced Composites: Materials, Manufacturing and Design*; Marcel Dekker Inc.: New York, 1993.
19. Majumdar, A.J.; Laws, V. *Glass Fiber Reinforced Cement*; BSP Professional Books: UK, 1991.
20. Beaudoin, J.J. *Handbook of Fiber-Reinforced Concrete: Principals, Properties, Developments and Applications*; Noyles Publications: Parkridge, N.J., 1990.
21. Bentur, A.; Mindness, S. *Fiber Reinforced Cementitious Composites*; Elsevier Science Publishers Ltd.: New York, 1990.